Journal of NeuroVirology, 15: 275–281, 2009

ISSN 1355-0284 print / 1538-2443 online
DOI: 10.1080/13550280902913271

informa
healthcare

Short communication

Serum matrix metalloproteinase levels correlate with brain injury in human immunodeficiency virus infection

Ann B Ragin,[1] Ying Wu,[1,2] Renee Ochs,[1] Rachel Scheidegger,[3] Bruce A Cohen,[4] Justin C McArthur,[5] Leon G Epstein,[6] and Katherine Conant[5]

[1]Department of Radiology, Northwestern University, Chicago, Illinois, USA; [2]Center for Advanced Imaging, North Shore Hospital, Evanston, Illinois, USA; [3]Harvard-MIT Division of Health Sciences and Technology, Cambridge, Massachusetts, USA; [4]Department of Neurology, Northwestern University, Chicago, Illinois, USA; [5]Department of Neurology, Johns Hopkins University, Baltimore, Maryland, USA; and [6]Division of Neurology, Children's Memorial Hospital, Chicago, Illinois, USA

Circulating levels of specific matrix metalloproteinases (MMPs; 1 and 7) were evaluated as correlates of brain injury in eight individuals in advanced human immunodeficiency virus (HIV) infection. Neurological status was quantified *in vivo* with automated segmentation algorithms and with diffusion tensor imaging. Both metalloproteinases correlated with microstructural brain alterations and the degree of atrophy. MMPs may influence neurological outcome through involvement in neuroimmune response, blood-brain barrier permeability, leukocyte migration, and MMP-mediated neurotoxicity. *Journal of NeuroVirology* (2009) **15,** 275–281.

Keywords: DTI; HIV dementia; MMP-1; MMP-7; neuroAIDS; segmentation

In human immunodeficiency virus (HIV) infection, there is considerable interest in the relationship of systemic factors to brain injury. The virus does not directly infect neurons and other markers of disease progression, such as CD4+ cell count, do not correspond to neurological outcome (Sevigny *et al,* 2004). In contrast, activated monocytes, measured in serum, correlate with dementia status (Pulliam *et al,* 1997). These findings have motivated efforts to determine factors in the systemic circulation that relate to the extent of injury to the brain. There is growing interest in the role of metalloproteinases (MMPs). This attention follows from evidence that MMPs are among the potentially neurotoxic products of monocyte-derived cells. Both MMP-1 and MMP-7, for example, are released from activated monocytes (Kouwenhoven *et al,* 2001).

The MMPs represent a family of endopeptidases involved in the processing of substrates, including soluble molecules, cell surface receptors, and extracellular matrix components, in both normal and pathological processes (Parks *et al*, 2004). MMPs are involved in pathogen clearance, monocyte migration, blood-brain barrier permeability, and neuroimmune processes. Emerging evidence suggests that MMPs may also contribute more directly to neuronal injury (Gu *et al*, 2002; Vos *et al*, 2000; Zhang *et al*, 2003). These enzymes interact with receptors expressed on neurons and involved in neuronal death (Conant *et al*, 2004). MMPs also generate toxic molecules from precursors expressed in the central nervous system (CNS) (Zhang *et al*, 2003).

In this investigation, serum levels of specific MMPs released from activated monocytes, including MMP-1 (collagenase-1) and MMP-7 (matrilysin) (Kouwenhoven *et al*, 2001), were evaluated for the degree of relationship to objective measurements of the brain, determined *in vivo* with quantitative

Address correspondence to Ann Ragin, Department of Radiology, 737 N. Michigan Avenue, #1600, Chicago, IL 60611-2927, USA. E-mail: ann-ragin@northwestern.edu

This work was supported by National Institutes of Health grants MH66705 (A.B.R.), MH080636 (A.B.R.), NS052580 (K.C.), and MH075673 (J.C.M.). The NEAD cohort was supported by NS044807 (J.C.M.) and NS049465 (J.C.M.). The authors thank Linda Reisberg, Pippa Storey, Alfred Shoukry, and the NEAD consortium.

Received 7 August 2008; revised 17 November; re-revised 4 February; accepted 9 March 2009.

magnetic resonance (MR) methodologies. Volumetric measurements of overall parenchyma and specific constituent tissue classes (white matter, gray matter, and cerebrospinal fluid [CSF]) were derived using automated brain segmentation algorithms (Smith *et al*, 2002). Measurements of aggregate microstructural brain alterations were derived with diffusion tensor imaging (DTI) (Basser and Pierpaoli, 1996). DTI exploits the random translational movements of water molecules as a noninvasive mechanism for probing tissue at a level that approximates cellular dimensions. Diffusion alterations have been identified in HIV-infected subjects (Filippi *et al*, 2001; Thurnher *et al*, 2005) and these measurements correlate with cognitive deficits (Ragin *et al*, 2004, 2005; Wu, 2006). MMP relationships were also determined for selected measures of immunological, virological, and cognitive (psychomotor, timed gait, and dementia severity) status.

Neuroradiological examinations were performed in eight well-characterized, medically stable subjects (six males, two females; mean age 52 ± 7.7) who were enrolled from a larger, longitudinal cohort study of neurological outcome in advanced HIV infection (e.g., Sevigny *et al*, 2004). Subjects had been followed in the larger, longitudinal cohort study with annual standardized clinical examinations, including comprehensive neurological/neuropsychological evaluations, as detailed in Sevigny *et al* (2004). Dementia severity was rated by a board-certified neurologist using an operationalized version of the Memorial Sloan Kettering (MSK) Staging for HIV-associated cognitive impairment. All subjects were in advanced infection meeting criteria for acquired immunodeficiency syndrome (AIDS) (average CD4 count $= 380 \pm 259.7$) and on antiretroviral regimens. Clinical and demographic characteristics of the sample are presented in Table 1. Study exclusion criteria included history of other neurological disorder, stroke, head trauma, opportunistic CNS infection, psychosis, or MR contraindication. Seropositivity was confirmed by enzyme-linked immunosorbent assay (ELISA) and Western blot. MMP-1 and MMP-7 levels were determined using commercial kits available through R&D Systems (Minneapolis, MN). Assays were performed according to the manufacturer's instructions.

Neuroradiologic examinations were performed on a 1.5-T twinspeed unit (Milwaukee, WI) with high-performance gradients using a quadrature birdcage headcoil for radiofrequency (RF) transmission and signal reception. T2- and proton density–weighted images were acquired using dual spin echo sequences, with repetition time (TR) = 3300 ms, echo times (TE) = 20 ms and 90 ms. Other parameters were as follows: flip angle: 90°; matrix size: 256×256; FOV: 24×18 cm; NEX = 2; slice thickness/gap: 3.5/0, 42 contiguous slices covering whole brain. DTI was performed with an echo planar sequence and bandwidth of ± 125 kHz. A b = 0 reference image and six diffusion-weighted images with a b-value of 1000 s/mm^2 were acquired at each slice location. The entire brain was imaged using 22 contiguous 7-mm axial sections (FOV: 24 cm; matrix size: 128×128; TR/NEX: 6200/4).

Quantitative image analysis was performed off-line. Image processing algorithms developed at Oxford University were used to determine the volumetric measurements (Smith *et al*, 2002; Zhang *et al*, 2001). These automated image analysis tools require minimal operator input. The normalized brain parenchymal volume, which adjusts for individual differences in brain size, was determined with SienaX based on T2-weighted images (Smith *et al*, 2002). Figure 1 illustrates segmentation of brain parenchyma and CSF, as shown in three dimensions. To calculate volume fractions of gray matter, white matter, and CSF, volume in mm^3 was determined for each tissue type and then divided by total brain volume, based on the T2- and proton density–weighted MR data (shown in Figure 2).

DTI measurements were calculated using customized image-processing routines written in MATLAB (Mathworks, Natick, MA). The background noise was first segmented from tissue by applying an automated thresholding technique to the diffusion-weighted images. This also removed voxels containing predominantly CSF, which have low intensity on diffusion-weighted images. To calculate the whole-brain DTI measurements, masks were generated at each brain level (Figure 3). Skin and

Table 1 Clincal characteristics

Subject	Age	Education	CD4	Nadir CD4*	Viral load	Avg. viral load*	CD8	BMI	Hemoglobin	MSK
1	45	12	367	108	152	756	1056	21.9	13.3	1
2	52	16	777	13	Lt 50	77494	1018	24.3	12.4	2
3	62	17	74	10	351	1014	684	21.4	13.5	1
4	41	14	737	176	Lt 50	24	1536	27.7	15.0	0
5	57	20	649	119	Lt 50	1853	1766	18.0	15.7	0
6	55	16	350	187	Lt 50	10245	1213	32.9	14.0	0
7	44	12	50	24	55300	57440	462	31.6	14.8	1
8	51	14	199	61	Lt 50	51963	1176	27.7	13.3	1

Note. MSK: Memorial Sloan Kettering Dementia Scale.
*Based on available clinical information for an average of 5 prior years.

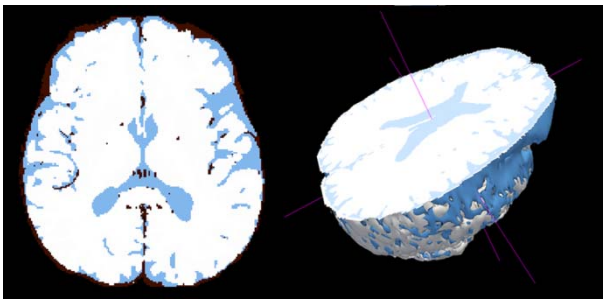

Figure 1 Parenchyma (*white*) is segmented from CSF (*blue*) to generate the brain parenchyma volume measure, as shown in a single axial slice. A partial 3D image of the brain is shown to illustrate that the voume is determined across the entire brain.

skull were removed based on a thresholding procedure. Manual editing was applied to refine the skull-stripping process. Reference points used for extraction of the brain mask were defined by manual operation. Mean diffusivity (MD) and fractional anisotropy (FA) were derived for each voxel across all brain levels according to standard equations (Basser and Pierpaoli, 1996). Histograms (Figure 3) were then generated and mean values of MD (in units of 10^{-3} mm^2/s) and of FA (which is dimensionless, ranging from 0 to 1) were determined for ''whole brain'' (i.e., across all nonmasked voxels).

Statistical analyses

Primary variables for analysis included serum MMP-1 and MMP-7 levels. Quantitative MR measurements included the normalized brain parenchyma volume (BPV) and volume fractions of gray matter, white matter, and cerebrospinal fluid (CSF). Microstructural measurements included mean diffusivity (MD) and fractional anisotropy (FA) derived for each subject from histograms (Figure 3) as described above. Clinical markers of disease progression included CD4 cell count and plasma HIV RNA copies/ml measured concurrently and averaged across the period of available clinical follow-up (approximately 5 years in this sample). Cognitive status measures included digit symbol, timed gait, and the ordinal Memorial Sloan Kettering HIV Dementia Rating Scale (MSK). For all variables, distributional assumptions were evaluated prior to analysis. Relationships of MMPs to variables of interest were determined using Pearson correlation coefficients or where indicated, the nonparametric equivalent, Spearman's rank. The significance level used for analyses was .05. Analyses were executed with SPSS (Chicago, IL).

MMP correlations with MR and clinical measures are shown in Table 2. Significant or nearly significant relationships were identified between the MMPs and segmentation-derived volumetric measurements: BPV (MMP-1: $r = -.80$; $P = .017$; MMP-7: $r = -.66$; $P = .070$) and CSF (MMP-1: $r = .67$; $P = .060$; MMP-7: $r = .69$; $P = .050$). Both MMPs were also significantly correlated with the whole-brain DTI measurements: MD (MMP-1: $r = .70$; $P = .050$; MMP-7: $r = .73$; $P = .040$) and FA (MMP-1: $r = -.72$; $P = .043$; MMP-7: $r = -.711$; $P = .048$). Examination of disease progression markers indicated no significant correlations between serum MMP levels and CD4 cell count or concurrent plasma HIV RNA copies/ml or MSK dementia rating. Elevated MMP-7, however, was significantly correlated with higher average HIV RNA copies/ml ($r = .75$; $P = .031$) and with poorer performance on a neuropsychological measure of psychomotor speed (digit symbol: $r = -.73$; $P = .040$). A nearly significant correlation was observed for elevated MMP-7 levels and slowed timed gait ($r = .63$; $P = .090$).

In this investigation, serum levels of MMP-1 and MMP-7 were evaluated as correlates of the degree of brain injury in subjects in advanced HIV infection. Elevated MMP levels were significantly correlated with brain atrophy, including reduced brain parenchyma volume and increased CSF, determined by

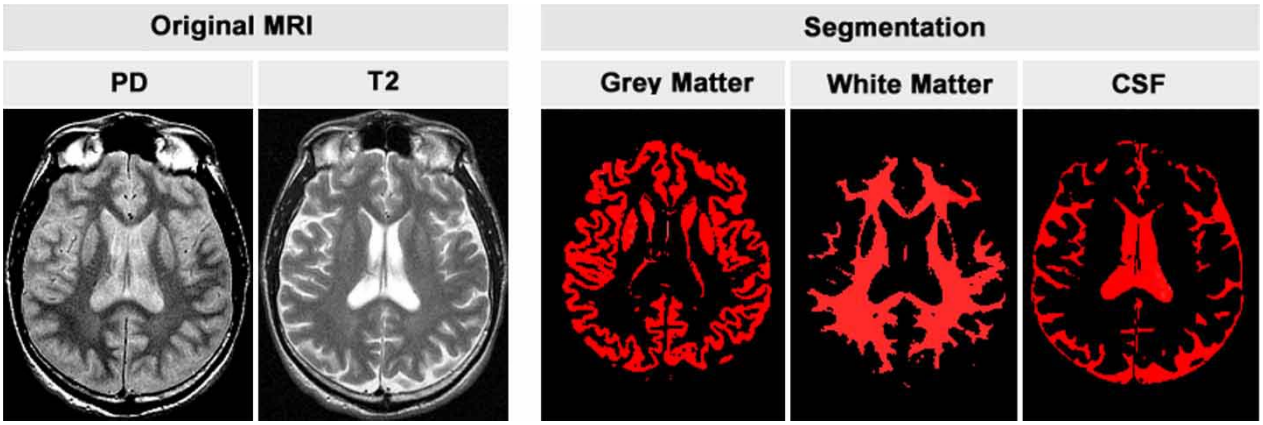

Figure 2 Proton density and T2 images in original gray scale (*left*) with segmentation of each tissue class (*right*) shown in red. Volume fractions are calculated across all slice levels.

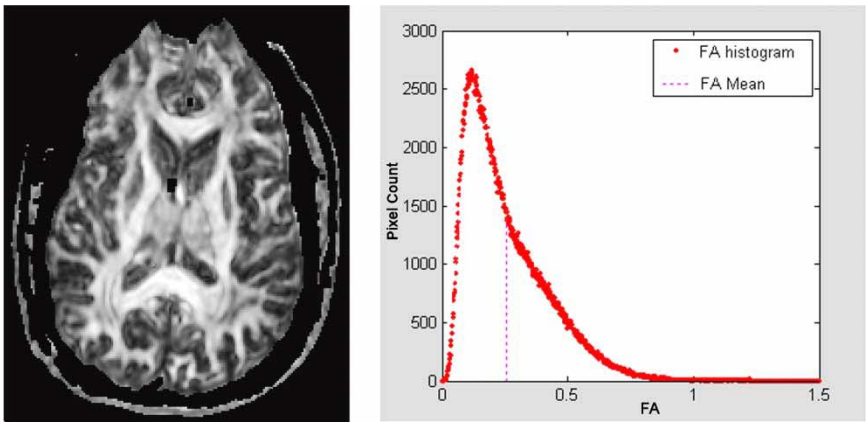

Figure 3 A representative FA map shown at the level of the interventricular foramen (*left*). FA is calculated for each voxel containing brain tissue. Thresholding and manual editing are used to remove voxels containing primarily CSF and skull. For each subject, a histogram of the resulting FA values is generated (*right*) and summarized as the histogram mean. The same approach was used to generate whole brain MD values.

automated segmentation algorithms. This pattern was mirrored at the microstructural level by two separate DTI measurements of aggregate sublethal alterations and tissue loss. Increased mean diffusivity reflects loss of barriers to diffusion (e.g., membranes) and expansion of the extracellular space resulting from changes such as neuronal loss. Reduced anisotropy is consistent with alterations in highly aligned cellular structures and loss of white matter integrity from changes such as axonal injury, glial cell swelling, astrocytosis, or hypertrophy of astrocytes.

Markers of progression in HIV infection, such as CD4+ cell count or viral replication in plasma, are not consistently associated with neurological outcome (Sevigny *et al*, 2004). In contrast, serum levels of activated monocytes in the circulation, as determined by surface expression of CD69, correlate with dementia status (Pulliam *et al,* 1997). The rationale for examining serum levels of MMPs follows from evidence that both MMP-1 and MMP-7 are released from activated monocytes (Kouwenhoven *et al*, 2001). Escalation in the trafficking of blood-borne activated monocytes from the bone marrow to the brain may be a critical determinant of HIV neurological injury. Converging lines of evidence implicate systemic monocyte activation and subsequent neuroinvasion in the neurological injury underlying cognitive deterioration in HIV infection (Gartner, 2000). Owing to facilitated brain ingress, activated monocytes traffic more readily into the brain, where they may deliver potentially neurotoxic products, including MMP-1 and MMP-7. The CD69-positive monocyte subset enter the brain, exposing neurons to these and other toxic factors (Pulliam *et al*, 1997). Products of activated monocytes released into the circulation may also enter the brain through altered integrity of the blood-brain barrier.

MMPs, which are tightly regulated at transcriptional and at post-translational levels, may be undetected in the healthy brain. Levels are elevated, however, in the CSF of subjects with HIV dementia (Conant *et al*, 1999), consistent with increased production and secretion by infiltrating cells (activated monocytes) and by cells intrinsic to the CNS (e.g., activated astrocytes, microglia, and neurons) (Yong *et al*, 1998). Although the significance of elevated MMPs in the vulnerable brain has not been fully characterized, it is clear that MMP dysregulation may pose considerable risk of tissue destruction. Matrix metalloproteinases are potent proteolytic enzymes that, considered collectively,

Table 2 Correlations of MMPs with MR and clinical variables

	MMP-1		MMP-7	
	r	*P*	*r*	*P*
Segmentation measurements				
White matter volume fraction	−.53	.17	−.56	.15
Gray matter volume fraction	−.40	.32	−.64	.09
CSF volume fraction	.67	.06	.70	.05
Brain parenchyma volume	−.80	.02	−.66	.08
DTI measurements				
Mean diffusivity	.70	.05	.73	.04
Fractional anisotropy	−.72	.04	−.71	.05
Clinical status measures				
CD4+ cell count	.36	.38	.48	.23
Concurrent HIV RNA	−.44	.27	−.00	.99
Average HIV RNA*	.00	.99	.75	.03
Cognitive status measures				
Psychomotor (digit symbol)	−.13	.76	−.73	.04
Timed gait	−.09	.83	.63	.09
MSK dementia rating	−.04	.93	.55	.16

Note. The data are Pearson correlation coefficients, except for ordinal scale MSK rating (Spearman).
*Based on available clinical information for an average of 5 prior years.

can degrade all constituents of the extracellular matrix (Sternlicht and Werb, 2001). MMPs may disrupt or degrade matrix proteins that support cell survival, cleave substrates to generate molecules that stimulate cell death, and act on cell surface receptors that influence cell survival.

In HIV infection, interactions of MMPs with cytokines, chemokines, and viral proteins may be of particular relevance to brain injury. MMPs studied in this investigation mediate conversion of cytokines implicated in HIV dementia, such as tumor necrosis factor alpha (TNFα) (Schlondorff and Blobel, 1999) and Fas ligand (FasL) (Lugli *et al*, 2005). MMPs may directly or indirectly alter the activity of cytokines and chemokines, potentiating neurotoxic effects. For example, stromal derived factor (SDF-1), a chemokine and substrate of MMP-1, is converted to a neurotoxic protein after MMP processing (Zhang *et al*, 2003). Implantation of cleaved SDF-1 into the basal ganglia results in inflammation and neuronal death in animal experiments (Zhang *et al*, 2003). MMP-1 also interacts with neuronal integrins to stimulate dephosphorylation of Akt and neuronal death through a nonproteolytic mechanism (Conant *et al*, 2004).

MMPs may modulate the neurotoxicity of HIV viral proteins (Johnston *et al*, 2001; Rumbaugh *et al*, 2006). Increased MMP-7 release and activation have been detected in cells expressing the HIV transactivating protein, Tat (Johnston *et al*, 2001). Some findings indicate *decreased* Tat-induced neurotoxicity and HIV transactivation, possibly owing to Tat's enzymatic cleavage by MMP-1 (Rumbaugh *et al*, 2006). This suggests that, at certain levels, MMPs may mediate neuroprotective/reparative processes or that the relative beneficial or detrimental role of MMPs may change across the clinical course. Prolonged activation of astrocytes has been shown to result in reduced levels of the endogeneous metalloproteinase inhibitor, TIMP-1, and sustained elevations of MMP-1 (Suryadevara *et al*, 2003). Reduced TIMP-1 levels have been identified in CSF and brain tissue from HIV dementia subjects (Dhar *et al*, 2006; Suryadevara *et al*, 2003). Taken together, this evidence suggests that the capacity of astrocytes to counter the potentially destructive effects of MMPs may diminish with chronic immune activation (Dhar *et al*, 2006).

In this investigation, MMP-7 was more closely related to virologic (average HIV RNA) and cognitive performance measures than MMP-1. There may be selective effects of MMP-1 and MMP-7 on the brain. MMPs typically target catalytic activity to specific substrates. Specific cell interactions have been reported for MMP-7 to surface proteoglycans (Yu and Woessner, 2000) and for MMP-1 to the α,β-integrin (Stricker *et al*, 2001). Cytokines implicated in HIV dementia, including TNFα and FasL, have been identified as substrates for MMP-7 (Haro *et al*, 2000; Powell *et al*, 1999). TNFα stimulation increases MMP-7 release by brain-derived cells (Conant *et al*, 1999). MMP-7 influences synaptic morphology (Bilousova *et al*, 2006; Patton *et al*, 1998) and neuronal survival (Bozzo *et al*, 1997) and is characterized by broad spectrum proteolytic activity against extracellular substrates, including proteoglycans, a major constituent of the extracellular matrix of the CNS, myelin, and TNFα; for a review, see Parks *et al* (2004).

Studies aimed at replicating and extending these findings may gain further insights by examining these MMPs in CSF specimens, which were not available for this sample. Analysis of metalloproteinase inhibitors (TIMPs) may also be informative. Although the expression of TIMPs may be up-regulated in response to some of the same stimuli that up-regulate the expression of MMPs, and although they can bind to and inhibit the activity of varied MMPs, increased MMP levels have nonetheless been linked to increased proteolysis of their substrates. The presence of inhibitors does not necessarily indicate that the MMP or all MMPs are inhibited. It is also possible that the inhibition occurs after the MMPs have already acted. Even if present for only a brief period prior to inactivation by TIMP binding or other mechanisms, MMPs may gain access to critical substrates. Moreover, MMP-7 lacks a hemopexin-like domain to which some TIMPs can bind.

It is important to appreciate that MMPs are among *many* products of activated monocytes that, following monocyte ingress into the brain parenchyma, may contribute to CNS damage. This study demonstrates the promising potential of quantitative imaging strategies for screening factors associated with HIV neurological injury. This imaging study, which is based on a small sample, indicates a consistent pattern of association between elevated MMP-1 and MMP-7 levels in the circulation and the severity of brain injury among individuals in advanced HIV infection. In particular, diffusion tensor imaging, which can be used to detect sublethal changes to the brain *in vivo*, may have considerable utility for evaluating the prognostic significance of MMPs and other factors as markers of neurological vulnerability earlier in the course of HIV infection.

Declaration of interest: The authors report no conflicts of interest. The authors alone are responsible for the content and writing of the paper.

References

Basser PJ, Pierpaoli C (1996). Microstructural and physiological features of tissues elucidated by quantitative-diffusion-tensor MRI. *J Magn Reson B* **111:** 209–219.

Bilousova TV, Rusakov DA, Ethell DW, Ethell IM (2006). Matrix metalloproteinase-7 disrupts dendritic spines in hippocampal neurons through NMDA receptor activation. *J Neurochem* **97:** 44–56.

Bozzo C, Bellomo G, Silengo L, Tarone G, Altruda F (1997). Soluble integrin ligands and growth factors independently rescue neuroblastoma cells from apoptosis under nonadherent conditions. *Exp Cell Res* **237:** 326–337.

Conant K, McArthur JC, Griffin DE, Sjulson L, Wahl LM, Irani DN (1999). Cerebrospinal fluid levels of MMP-2, 7, and 9 are elevated in association with human immunodeficiency virus dementia. *Ann Neurol* **46:** 391–398.

Conant K, St Hillaire C, Nagase H, Visse R, Gary D, Haughey N, Anderson C, Turchan J, Nath A (2004). Matrix metalloproteinase 1 interacts with neuronal integrins and stimulates dephosphorylation of Akt. *J Biol Chem* **279:** 8056–8062.

Dhar A, Gardner J, Borgmann K, Wu L, Ghorpade A (2006). Novel role of TGF-beta in differential astrocyte-TIMP-1 regulation: implications for HIV-1-dementia and neuroinflammation. *J Neurosci Res* **83:** 1271–1280.

Filippi CG, Ulug AM, Ryan E, Ferrando SJ, van Gorp W (2001). Diffusion tensor imaging of patients with HIV and normal-appearing white matter on MR images of the brain [see comment]. *AJNR Am J Neuroradiol* **22:** 277–283.

Gu Z, Kaul M, Yan B, Kridel SJ, Cui J, Strongin A, Smith JW, Liddington RC, Lipton SA (2002). S-nitrosylation of matrix metalloproteinases: signaling pathway to neuronal cell death. *Science* **297:** 1186–1190.

Haro H, Crawford HC, Fingleton B, Shinomiya K, Spengler DM, Matrisian LM (2000). Matrix metalloproteinase-7-dependent release of tumor necrosis factor-alpha in a model of herniated disc resorption. *J Clin Invest* **105:** 143–150.

Johnston JB, Zhang K, Silva C, Shalinsky DR, Conant K, Ni W, Corbett D, Yong VW, Power C (2001). HIV-1 Tat neurotoxicity is prevented by matrix metalloproteinase inhibitors. *Ann Neurol* **49:** 230–241.

Kouwenhoven M, Ozenci V, Gomes A, Yarilin D, Giedraitis V, Press R, Link H (2001). Multiple sclerosis: elevated expression of matrix metalloproteinases in blood monocytes. *J Autoimmun* **16:** 463–470.

Lugli E, Pinti M, Nasi M, Troiano L, Prada N, Mussini C, Borghi V, Esposito R, Cossarizza A (2005). MMP-7 promoter polymorphisms do not influence CD4+ recovery and changes in plasma viral load during antiretroviral therapy for HIV-1 infection. *Int J Immunogenet* **32:** 269–271.

Parks WC, Wilson CL, Lopez-Boado YS (2004). Matrix metalloproteinases as modulators of inflammation and innate immunity. *Nat Rev Immunol* **4:** 617–629.

Patton BL, Chiu AY, Sanes JR (1998). Synaptic laminin prevents glial entry into the synaptic cleft. *Nature* **393:** 698–701.

Powell WC, Fingleton B, Wilson CL, Boothby M, Matrisian LM (1999). The metalloproteinase matrilysin proteoly tically generates active soluble Fas ligand and potentiates epithelial cell apoptosis. *Curr Biol* **9:** 1441–1447.

Pulliam L, Gascon R, Stubblebine M, McGuire D, McGrath MS (1997). Unique monocyte subset in patients with AIDS dementia. *Lancet* **349:** 692–695.

Ragin AB, Storey P, Cohen BA, Edelman RR, Epstein LG (2004). Disease burden in HIV-associated cognitive impairment: a study of whole-brain imaging measures. *Neurology* **63:** 2293–2297.

Ragin AB, Wu Y, Storey P, Cohen BA, Edelman RR, Epstein LG (2005). Diffusion tensor imaging of subcortical brain injury in patients infected with human immunodeficiency virus. *J NeuroVirol* **11:** 292–298.

Rumbaugh J, Turchan-Cholewo J, Galey D, St Hillaire C, Anderson C, Conant K, Nath A (2006). Interaction of HIV Tat and matrix metalloproteinase in HIV neuropathogenesis: a new host defense mechanism. *FASEB J* **20:** 1736–1738.

Schlondorff J, Blobel CP (1999). Metalloprotease-disintegrins: modular proteins capable of promoting cell-cell interactions and triggering signals by protein-ectodomain shedding. *J Cell Sci* **112 (Pt 21):** 3603–3617.

Sevigny JJ, Albert SM, McDermott MP, McArthur JC, Sacktor N, Conant K, Schifitto G, Selnes OA, Stern Y, McClernon DR, Palumbo D, Kieburtz K, Riggs G, Cohen B, Epstein LG, Marder K (2004). Evaluation of HIV RNA and markers of immune activation as predictors of HIV-associated dementia. *Neurology* **63:** 2084–2090.

Smith SM, Zhang Y, Jenkinson M, Chen J, Matthews PM, Federico A, De Stefano N (2002). Accurate, robust, and automated longitudinal and cross-sectional brain change analysis. *Neuroimage* **17:** 479–489.

Sternlicht MD, Werb Z (2001). How matrix metalloproteinases regulate cell behavior. *Annu Rev Cell Dev Biol* **17:** 463–516.

Stricker TP, Dumin JA, Dickeson SK, Chung L, Nagase H, Parks WC, Santoro SA (2001). Structural analysis of the alpha(2) integrin I domain/procollagenase-1 (matrix metalloproteinase-1) interaction. *J Biol Chem* **276:** 29375–29381.

Suryadevara R, Holter S, Borgmann K, Persidsky R, Labenz-Zink C, Persidsky Y, Gendelman HE, Wu L, Ghorpade A (2003). Regulation of tissue inhibitor of metalloproteinase-1 by astrocytes: links to HIV-1 dementia. *Glia* **44:** 47–56.

Thurnher MM, Castillo M, Stadler A, Rieger A, Schmid B, Sundgren PC (2005). Diffusion-tensor MR imaging of the brain in human immunodeficiency virus-positive patients. *AJNR Am J Neuroradiol* **26:** 2275–2281.

Vos CM, Sjulson L, Nath A, McArthur JC, Pardo CA, Rothstein J, Conant K (2000). Cytotoxicity by matrix metalloprotease-1 in organotypic spinal cord and dissociated neuronal cultures. *Exp Neurol* **163:** 324–330.

Wu Y, Storey P, Cohen BA, Epstein LG, Edelman RR, Ragin AB (2006). Diffusion alterations in corpus callosum of patients with HIV. *AJNR Am J Neuroradiol* **27**: 656–660.

Yong VW, Krekoski CA, Forsyth PA, Bell R, Edwards DR (1998). Matrix metalloproteinases and diseases of the CNS. *Trends Neurosci* **21:** 75–80.

Yu WH, Woessner JF Jr (2000). Heparan sulfate proteoglycans as extracellular docking molecules for matrilysin (matrix metalloproteinase 7). *J Biol Chem* **275:** 4183–4191.

Zhang K, McQuibban GA, Silva C, Butler GS, Johnston JB, Holden J, Clark-Lewis I, Overall CM, Power C (2003). HIV-induced metalloproteinase processing of the chemokine stromal cell derived factor-1 causes neurodegeneration. *Nat Neurosci* **6:** 1064–1071.

Zhang Y, Brady M, Smith S (2001). Segmentation of brain MR images through a hidden Markov random field model and the expectation-maximization algorithm. *IEEE Trans Med Imaging* **20:** 45–57.

This paper was first published online on iFirst on 13 May 2009.